Coordinated Regulation of Palladin and α–Smooth Muscle Actin by Transforming Growth Factor–β in Human Corneal Fibroblasts

Naoyuki Morishige, Shizuka Murata, Yoshikuni Nakamura, Haruya Azumi, Ryutaro Shin-gyou-uchi, Ken-Taro Oki, Yukiko Morita, and Koh-Hei Sonoda

Department of Ophthalmology, Yamaguchi University Graduate School of Medicine, Ube, Yamaguchi, Japan

Correspondence: Naoyuki Morishige, Department of Ophthalmology, Yamaguchi University Graduate School of Medicine, 1-1-1 Minami Kogushi, Ube, Yamaguchi 755-8505, Japan;
morishig@yamaguchi-u.ac.jp.

NM and SM contributed equally to the work presented here and should therefore be regarded as equivalent authors.

Submitted: November 29, 2015
Accepted: May 9, 2016

Citation: Morishige N, Murata S, Nakamura Y, et al. Coordinated regulation of palladin and α–smooth muscle actin by transforming growth factor–β in human corneal fibroblasts. *Invest Ophthalmol Vis Sci*. 2016;57:3360–3368. DOI:10.1167/iovs.15-18763

Purpose. To investigate the role of palladin in the cornea, we examined expression of this actin assembly–related protein in normal, diseased, or injured corneal tissue as well as in cultured corneal fibroblasts.

Methods. Expression of palladin and α–smooth muscle actin (α-SMA) in the rat cornea with an incision wound, in the normal and diseased human cornea, and in cultured human corneal fibroblasts was examined by immunofluorescence or immunoblot analysis.

Results. The expression of both palladin and α-SMA was detected at the lesion site during wound healing in the rat cornea. Whereas neither palladin nor α-SMA was detected in the normal human cornea, the colocalization of both proteins was detected in diseased human corneas with underlying conditions characterized by the presence of fibrosis. The expression of both palladin and α-SMA in cultured human corneal fibroblasts was increased by transforming growth factor–β (TGF-β) in a manner sensitive to inhibition by blockers of Smad or mitogen-activated protein kinase (MAPK) signaling. Finally, RNA interference–mediated depletion of palladin attenuated the TGF-β–induced upregulation of α-SMA expression in human corneal fibroblasts as well as TGF-β–induced collagen gel contraction mediated by these cells.

Conclusions. Palladin is expressed in the rat and human cornea in association with scar formation. Expression of palladin in human corneal fibroblasts is increased by TGF-β in a manner dependent on Smad and MAPK signaling and is required for the TGF-β–induced upregulation of α-SMA.

Keywords: palladin, TGFb, alpha-smooth muscle actin, corneal fibroblasts

The stroma accounts for ~90% of the thickness of the human cornea and is composed of keratocytes and an extracellular matrix consisting largely of collagen and proteoglycans. The stability of the corneal stroma is critical for maintenance of corneal transparency. Various diseases or injury can disrupt stromal stability, however, and lead to the development of corneal scarring. Keratocytes play an important role in the process of stromal scarring by undergoing a change in phenotype through transdifferentiation into fibroblasts and myofibroblasts that express α–smooth muscle actin (α-SMA).[1,2] The expression of α-SMA is regulated by various growth factors—including transforming growth factor–β (TGF-β),[1] platelet-derived growth factor,[1,3] and basic fibroblast growth factor[4]—through various signaling pathways including those mediated by Smad family, the mitogen-activated protein kinases (MAPKs) p38, c-Jun N-terminal kinase (JNK), and ERK (extracellular signal–regulated kinase).[5–10] Myofibroblasts in the cornea secrete abnormal collagen molecules that disrupt the oriented structure of collagen fibers in the stroma and thereby diminish corneal transparency.[11–13] Furthermore, the transparency of myofibroblasts themselves is reduced compared with that of keratocytes.[14,15] Myofibroblasts expressing α-SMA are thus key players in the loss of corneal transparency associated with the development of scar lesions such as those due to trauma,[16] refractive surgery,[17,18] or bullous keratopathy.[19,20]

Palladin is a member of a cytoskeletal protein family that includes myotilin and myopalladin,[21–24] and it is widely expressed in epithelial and mesenchymal tissues.[25] Palladin interacts with several actin-associated proteins including α-actinin, VASP, ArgBP2, and profilin and thereby serves as a molecular scaffold to organize and stabilize the actin cytoskeleton.[24,26–29] Indeed, downregulation of palladin expression has been found to induce disruption of actin stress fibers.[22,29–31] Palladin is expressed in myofibroblasts of the stroma of solid tumors, and it is thought to promote the migration of these cells and thereby to facilitate tumor cell invasion.[32,33] Indeed, palladin may serve as a marker for cancer-associated myofibroblasts.[34] These observations suggest that palladin might also play an important role in corneal myofibroblasts, in which actin stress fibers have been shown to be abundant both in vitro and in vivo.[5]

We have now investigated the expression of palladin in the normal, diseased, or injured corneal stroma. In addition, we examined the role of TGF-β in the regulation of palladin expression in corneal fibroblasts as well as the effect of palladin depletion by RNA interference (RNAi) on the TGF-β–induced expression of α-SMA in these cells. Our data suggest that

Investigative Ophthalmology & Visual Science

palladin plays a key role in myofibroblast transdifferentiation and thereby contributes to corneal stromal scarring.

Methods

Rat Model of Corneal Stromal Wound Healing

All animal experiments were performed in accordance with the ARVO Statement for the Use of Animals in Ophthalmic and Vision Research and were approved by the animal ethics committee of Yamaguchi University Graduate School of Medicine. Wistar rats (8 weeks of age) were obtained from SLC (Shizuoka, Japan). The animals were anesthetized by intraperitoneal injection of sodium pentobarbital (30 mg/kg body mass) and by application of 0.4% oxybuprocain hydrochloride to the right eye. A sharp incision to a depth of 150 μm was made in the right eye with the use of a diamond knife, and the animals were killed by cervical dislocation either 24 hours, 48 hours, 72 hours, 1 week, or 2 weeks later. The right eye was enucleated, immediately frozen in optimum cutting temperature (OCT) compound (Sakura Finetechnical, Tokyo, Japan), and stored at −80°C until preparation of cryosections.

Human Corneal Specimens

Human tissue was used in strict accordance with the tenets of the Declaration of Helsinki and with approval of the Institutional Review Board of Yamaguchi University Hospital. Normal corneal buttons (derived from four male donors and one female donor with a mean age ± SD of 51.2 ± 8.3 years and age range of 39–57 years) were obtained from Sight Life Eye Bank (Seattle, WA, USA). Corneal buttons from four individuals with bullous keratopathy, four with corneal leukoma due to interstitial keratitis, one with corneal leukoma due to bacterial ulcerative keratitis, and one with keratoconus (total of two men and eight women with a mean age ± SD of 65.5 ± 21.8 years and age range of 18–88 years) were obtained at the time of keratoplasty performed at Yamaguchi University Hospital. The specimens were treated and sectioned as described above.

Isolation and Culture of Human Corneal Fibroblasts

Four human corneas for penetrating keratoplasty were obtained from Sight Life Eye Bank. The donors were white men and women ranging in age from 52 to 75 years. After the center of each donor cornea was excised for keratoplasty, the epithelium and endothelium were removed from the remaining sclerocorneal rim, the stroma was separated from the sclera, and the stromal tissue was digested overnight at 37°C with collagenase (2.0 mg/mL) (Invitrogen, Carlsbad, CA, USA) and hyaluronidase (0.5 mg/mL) (Worthington Biochemical, Freehold, NJ, USA) in sterile minimum essential medium (MEM) (Invitrogen). The stromal cells were then isolated by centrifugation, and the cells from each cornea were cultured separately in 60-mm dishes containing MEM supplemented with 10% fetal bovine serum (FBS) (Gibco, Carlsbad, CA, USA) until they had achieved ∼90% confluence. The purity of the cell cultures was judged on the basis of both the distinctive morphology of corneal fibroblasts and their reactivity with antibodies to vimentin in immunofluorescence analysis.[35] No contamination with corneal epithelial cells was detected. The human corneal fibroblasts (HCFs) were used for experiments after four to six passages.

Immunofluorescence Microscopy

Cryosectioned tissue samples were fixed with 4% paraformaldehyde, permeabilized with ice-cold acetone, exposed to 3% bovine serum albumin in phosphate-buffered saline, and incubated for 1 hour at room temperature with mouse monoclonal antibodies to palladin (Novus, Littleton, CO, USA) or rabbit polyclonal antibodies to α-SMA (Abcam, Cambridge, UK). The sections were washed and then incubated for 1 hour at room temperature with fluorescein isothiocyanate (FITC)–conjugated goat antibodies to rabbit or mouse immunoglobulin G (Invitrogen), with Alexa Fluor 633–conjugated antibodies to rabbit immunoglobulin G (Invitrogen), with Syto 59 (Invitrogen), or with rhodamine-phalloidin (Invitrogen). Human corneal fibroblasts cultured in glass-bottom dishes were fixed with ice-cold acetone, exposed to 3% bovine serum albumin in phosphate-buffered saline, and incubated for 1 hour at room temperature with mouse monoclonal antibodies to palladin (Novus). The cells were washed and then incubated for 1 hour at room temperature with FITC-conjugated rabbit polyclonal antibodies to mouse immunoglobulin G (Invitrogen) and with rhodamine-phalloidin. Tissue sections and cells were then observed and imaged with a laser scanning confocal microscope (LSM Pascal; Carl Zeiss Microimaging, Jena, Germany).

Analysis of the Effect of TGF-β on Palladin Expression in HCFs

Human corneal fibroblasts at ∼90% confluence were deprived of serum for 24 hours by incubation in Dulbecco's modifed Eagle's medium (DMEM) (Invitrogen) supplemented with 1% RPMI vitamin mix (Sigma-Aldrich, Corp., St. Louis, MO, USA), nonessential amino acids (Invitrogen), L-ascorbic acid 2-phosphate (289 μg/mL) (Sigma-Aldrich, Corp.), and 1% penicillin–streptomycin–amphotericin B (Invitrogen). The cells were then incubated for 24, 48, or 72 hours in serum-free MEM containing various concentrations (0.1–10 ng/mL) of recombinant human TGF-β1 (R&D Systems, Minneapolis, MN, USA) before lysis in RIPA buffer (50 mM Tris-HCl [pH 7.5], 150 mM NaCl, 5 mM $MgCl_2$, 0.25% SDS, 0.25% sodium deoxycholate, 1% Nonidet P-40, 100 mM NaF, 100 mM sodium orthovanadate, 1 mM EGTA, 1 mM EDTA) containing a proteinase inhibitor cocktail (Sigma-Aldrich, Corp.). The cell lysates were subjected to immunoblot analysis.

Analysis of the Effects of MAPK Signaling Inhibitors on TGF-β–Induced Palladin Expression in HCFs

Cells deprived of serum for 24 hours were incubated first for 1 hour in serum-free MEM containing 30 μM PD98059 (an inhibitor of ERK signaling) (Calbiochem, Darmstadt, Germany), 10 μM SB203580 (an inhibitor of p38 signaling) (Calbiochem), 3 μM SP600125 (an inhibitor of JNK signaling) (Wako Pure Chemical Industries, Osaka, Japan), or 1 μM SB525334 (an inhibitor of Smad2/3) (Wako Pure Chemical Industries) and then for 23 hours in the additional absence or presence of TGF-β (10 ng/mL). Cell lysates were then prepared for immunoblot analysis as described above.

Immunoblot Analysis

Cell lysates were fractionated by SDS-polyacrylamide gel electrophoresis, and the separated proteins were transferred to a nitrocellulose membrane. The membrane was then incubated with rabbit polyclonal antibodies to α-SMA (Sigma-Aldrich, Corp.) or mouse monoclonal antibodies to palladin (Novus), after which immune complexes were detected with

Investigative Ophthalmology & Visual Science

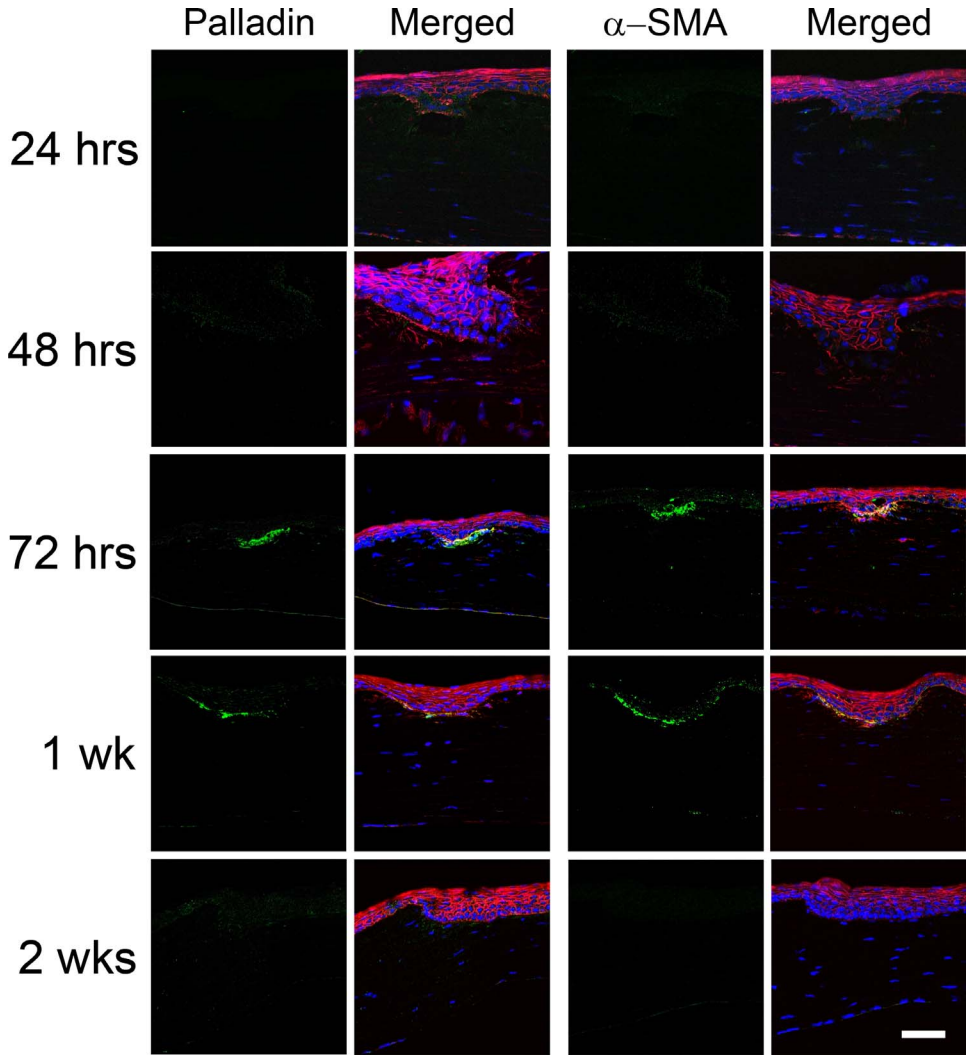

FIGURE 1. Immunohistofluorescence analysis of the expression of palladin and α-SMA in a rat model of corneal stromal wound healing. Corneal sections prepared at the indicated times after incisional wounding were stained with antibodies to palladin or to α-SMA (*green fluorescence*). Merged images also show staining with rhodamine-phalloidin to detect the actin cytoskeleton (*red fluorescence*) and with Syto 59 to detect nuclei (*blue fluorescence*). *Scale bar*: 50 μm.

horseradish peroxidase–conjugated secondary antibodies and enhanced chemiluminescence reagents (Amersham–GE Healthcare, Little Chalfont, UK).

RNA Interference

Human corneal fibroblasts at ~80% confluence were isolated and transferred to six-well plates (for RT-PCR or immunoblot analysis) or to 35-mm glass-bottom dishes (for immunofluorescence analysis) containing antibiotic-free Transfection Medium (Santa Cruz Biotechnology, Dallas, TX, USA). The cells were then transfected for 6 hours with palladin (sc88986, Santa Cruz Biotechnology) or control (sc37007, Santa Cruz Biotechnology) small interfering RNAs (siRNAs), incubated for 24 hours in MEM supplemented with 10% FBS, and stimulated with TGF-β (10 ng/mL) in serum-free medium for 12 hours (for RT-PCR analysis) or 48 hours (for immunoblot or immunofluorescence analysis).

RT-PCR Analysis

Human corneal fibroblasts were washed with phosphate-buffered saline, and total RNA was extracted from the cells and subjected to reverse transcription (RT) with the use of an RNeasy Mini Kit (Qiagen, Valencia, CA, USA) and a Reverse Transcription System (Promega, Fitchburg, WI, USA), respectively. The abundance of palladin and α-SMA mRNAs was quantified by real-time polymerase chain reaction (PCR) analysis with the use of a LightCycler instrument (Roche Diagnostics, Mannheim, Germany). Transcripts of the constitutively expressed gene for glyceraldehyde-3-phosphate dehydrogenase (GAPDH) served to normalize the amount of palladin and α-SMA mRNAs in each sample. The sequences of the PCR primers (sense and antisense, respectively) were 5′-CTGCCCAAGGGTGTCAC-3′ and 5′-CTTTGGCTTTGGATTTCCAG-3′ for palladin, 5′-AGGAAGGACCTCTATGCTAACAAT-3′ and 5′-AACACATAGGTAACGAGTCAGAGC-3′ for α-SMA, and 5′-TGAACGGGAAGCTCACTGG-3′ and 5′-TCCACCACCCTGTTGCTGTA-3′ for GAPDH. The PCR protocol comprised an initial denaturation step at 95°C for 30 seconds followed by 40 cycles of amplification. For the amplification of palladin cDNA, the cycles consisted of denaturation at 95°C for 15 seconds, annealing at 59°C for 10 seconds, and elongation at 72°C for 10 seconds. For the amplification of α-SMA cDNA, the cycles included denaturation at 95°C for 10 seconds, annealing at

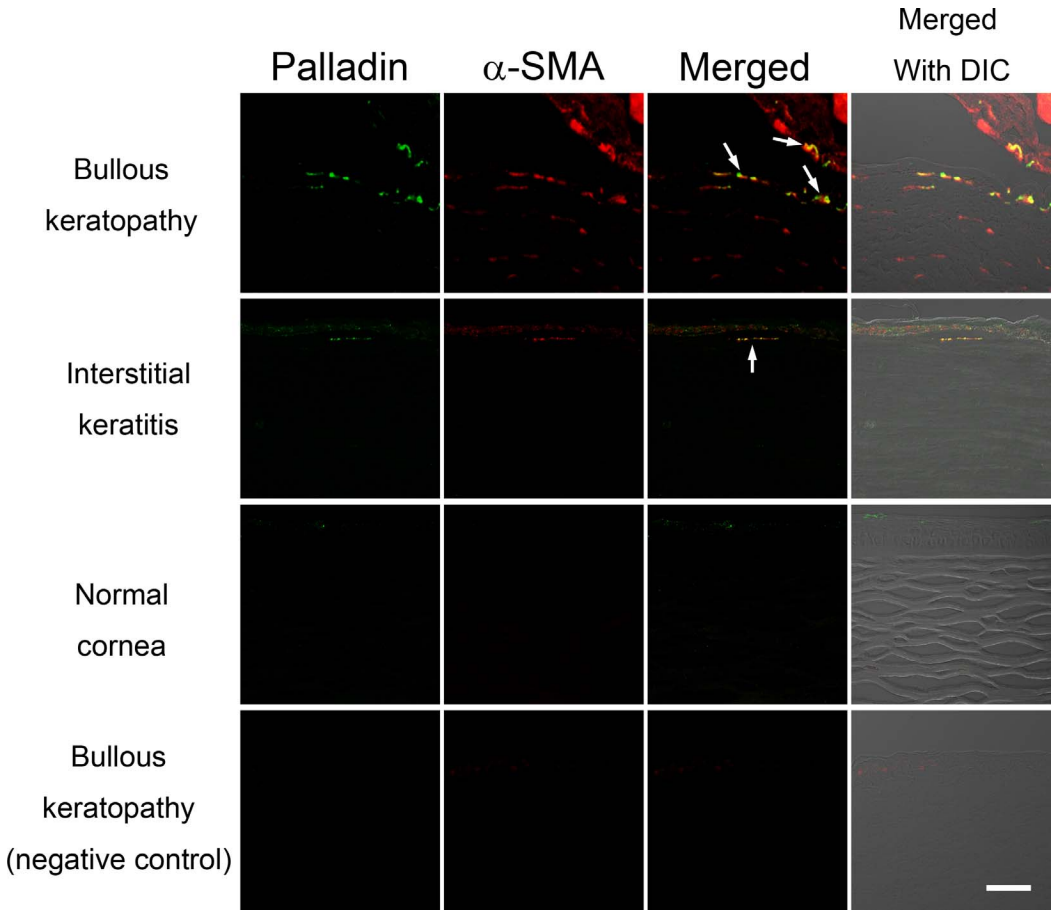

FIGURE 2. Immunohistofluorescence analysis of the expression of palladin and α-SMA in normal and diseased human corneas. Specimens of the human cornea affected by bullous keratopathy (*top and bottom rows*) or by leukoma due to syphilitic interstitial keratitis (*second row*), or of a normal human cornea (*third row*), were stained with antibodies to palladin (*green fluorescence*) and those to α-SMA *(red fluorescence*) or with corresponding control nonspecific antibodies (negative control). Merged immunofluorescence images as well as merged immunofluorescence and differential interference contrast (DIC) microscopic images are also shown. *Arrows* indicate colocalization of palladin and α-SMA. *Scale bar*: 50 μm.

55°C for 10 seconds, and elongation at 72°C for 25 seconds. For the amplification of GAPDH cDNA, the cycles consisted of denaturation at 95°C for 15 seconds, annealing at 55°C for 10 seconds, and elongation at 72°C for 20 seconds. Real-time PCR data were analyzed with the use of LightCycler software 3.01 (Roche Diagnostics, Mannheim, Germany).

Collagen Gel Contraction Assay

Human corneal fibroblasts transfected with palladin or control siRNAs for 6 hours as described above were incubated for 24 hours in MEM supplemented with 10% FBS and then suspended in serum-free MEM at a density of 1.1×10^7/mL. Type I collagen (Nitta Gelatin, Osaka, Japan), reconstitution buffer (Nitta Gelatin), 10× MEM (Invitrogen), and HCF suspension were mixed on ice in a volume ratio of 7:1:1:1 (final concentration of type I collagen, 2.1 mg/mL; final cell density, 1.0×10^6/mL). A portion (0.5 mL) of the mixture was added to each well of a 24-well plate, which was then placed for 30 minutes in a 37°C incubator containing 5% CO_2 to induce gel formation. Minimum essential medium (0.5 mL) with or without TGF-β (10 ng/mL) was added on top of each collagen gel; the plate was placed in the incubator for 1 hour, and each gel was then freed from the sides of the well with the use of a microspatula. The gels were then cultured for 4 days, and the diameter of each gel was measured with a ruler every 24 hours.

Statistical Analysis

Quantitative data are presented as means ± SEM and were compared among four groups with analysis of variance (ANOVA) followed by the Tukey test as performed with SPSS version 21 software (IBM, Armonk, NY, USA). A P value < 0.05 was considered statistically significant.

RESULTS

Palladin Expression in a Rat Model of Corneal Stromal Wound Healing and in the Normal and Diseased Human Cornea

Given that, as far as we are aware, the expression of palladin in corneal tissue has not previously been described, we first examined the expression of this protein as well as that of α-SMA in a rat model of stromal wound healing. Neither palladin nor α-SMA was detected in the cornea at 24 or 48 hours after incisional injury (Fig. 1). From 72 hours through 1 week after wounding, however, the expression of palladin was detected at the base of the incision, in a region below epithelial cells that also manifested α-SMA expression. The expression of both palladin and α-SMA was no longer apparent in the cornea at 2 weeks after injury.

TABLE. Characteristics of the Human Corneal Specimens Evaluated for Expression of Palladin and α-SMA

Age, Years, Sex	Disease	Background Condition	Expression of		Colocalization
			α-SMA	Palladin	
70/F	BK	Post ICCE	+	+	+
18/F	BK	Post ICCE	+	+	+
78/F	BK	Laser iridotomy	−	−	
78/M	BK	Pseudoexfoliation	+	+	+
88/F	Leukoma	Syphilitic	+	+	+
79/F	Leukoma	Syphilitic	−	−	
71/F	Leukoma	Herpetic	+	+	+
70/F	Leukoma	Herpetic	−	−	
67/F	Leukoma	Bacterial infection	+	+	−
41/M	Keratoconus	Acute hydrops	+	+	−
57/M	Normal		−	−	
57/F	Normal		−	−	
39/M	Normal		−	−	
46/M	Normal		−	−	
57/M	Normal		−	−	

BK, bullous keratopathy; ICCE, intracapsular cataract extraction.

Immunofluorescence microscopy also revealed the apparent absence of both palladin and α-SMA expression in specimens of normal human corneas (Fig. 2; Table). Palladin immunoreactivity was detected together with α-SMA in the anterior stroma of three out of four corneas affected by bullous keratopathy, two out of four corneas with leukoma due to interstitial keratitis, one cornea with leukoma due to ulcerative keratitis, and one cornea with keratoconus (Fig. 2; Table). In the positive specimens affected by bullous keratopathy or corneal leukoma due to interstitial keratitis, α-SMA and palladin were detected in the same cells. Together, these observations of the rat and human cornea suggested that the expression of palladin may be related to that of α-SMA in corneal scar lesions.

Effect of TGF-β on Palladin Expression in Cultured HCFs

Given that TGF-β is implicated in corneal scarring,[17] we next investigated the possible effect of this growth factor on the expression of palladin in HCFs. Immunoblot analysis revealed that exposure of HCFs to TGF-β for 72 hours increased the abundance of palladin as well as that of α-SMA in a concentration-dependent manner, with the effect on the 140-kDa isoform of palladin being more pronounced than that on the 90-kDa isoform (Fig. 3A). The effects of TGF-β (10 ng/mL) on palladin and α-SMA expression were also time dependent, being apparent at 24 hours, maximal at 48 hours, and still evident at 72 hours (Fig. 3B).

We next investigated the possible role of Smad or MAPK signaling pathways in the upregulation of palladin expression by TGF-β, given that such signaling has been implicated in the induction of α-SMA expression by TGF-β.[36–38] The TGF-β–induced increase in the abundance of the 140-kDa isoform of palladin as well as that in the amount of α-SMA was attenuated in the presence of the ERK signaling inhibitor PD98059, the p38 inhibitor SB203580, the JNK inhibitor SP600125, or Smad 2/3 inhibitor SB525334 (Fig. 4). The effect of SB525334 as well as SP600125 on the TGF-β–induced upregulation of the 140-kDa isoform of palladin was more pronounced than that of SB203580 or PD98059. Further, the two inhibitors of SP600125 and SB525334 had a marked effect on expression of the 90-kDa isoform of paladin compared to PD98059 or SB203580. These results thus suggested that the TGF-β–induced upregulation of the 140-kDa isoform of palladin, similar to that of α-SMA, is mediated at least in part by Smad, ERK, p38 MAPK, and JNK signaling pathways.

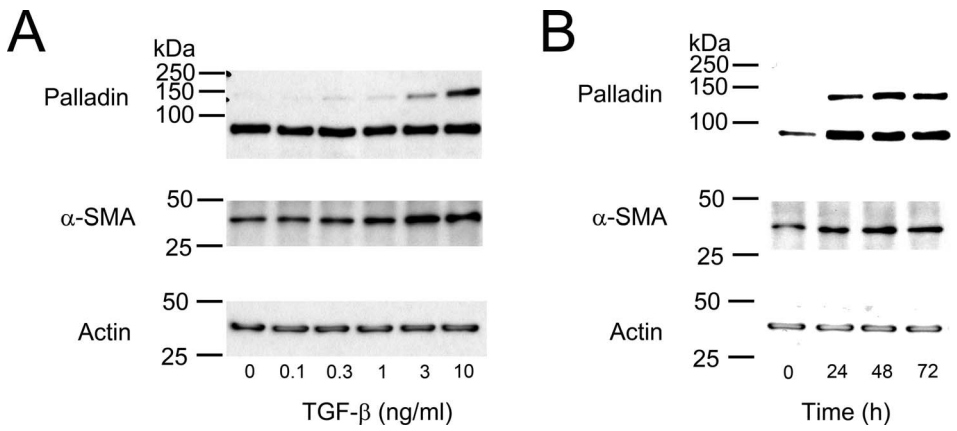

FIGURE 3. Concentration- and time-dependent effect of TGF-β on palladin expression in HCFs. HCFs were incubated in the presence of the indicated concentrations of TGF-β for 72 hours (**A**) or in the presence of TGF-β (10 ng/mL) for the indicated times (**B**), after which cell lysates were prepared and subjected to immunoblot analysis with antibodies to palladin, to α-SMA, or to β-actin (loading control).

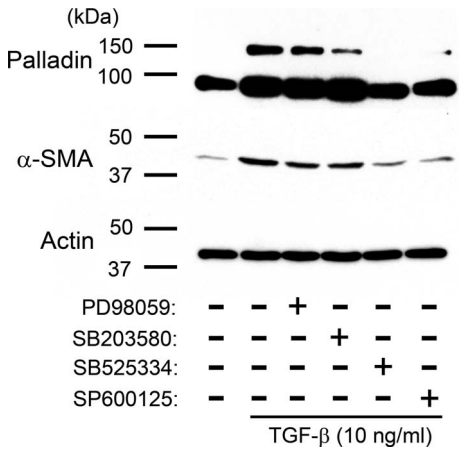

FIGURE 4. Effects of Smad and MAPK signaling inhibitors on the TGF-β–induced upregulation of palladin expression in HCFs. HCFs were incubated in the absence or presence of 30 μM PD98059, 10 μM SB203580, 1 μM SB525334, or 3 μM SP600125 for 1 hour and then in the additional absence or presence of TGF-β (10 ng/mL) for 23 hours, after which cell lysates were prepared and subjected to immunoblot analysis with antibodies to paladin, to α-SMA, or to actin.

Role of Palladin in the TGF-β–Induced Upregulation of α-SMA Expression in HCFs

We examined the effect of RNA-mediated depletion of palladin on the expression of α-SMA in HCFs. Immunofluorescence analysis confirmed that the expression of palladin in TGF-β–treated HCFs was attenuated by transfection with a palladin siRNA, whereas the morphology of the cells did not appear to be affected by palladin depletion (Fig. 5A). Quantitative RT-PCR analysis revealed that the abundance of palladin and α-SMA mRNAs in TGF-β–treated HCFs was reduced by 55.6% and 22.1%, respectively, as a result of transfection with the palladin siRNA (Fig. 5B). Immunoblot analysis revealed that the TGF-β–induced upregulation of α-SMA, as well as that of both 140- and 90-kDa isoforms of paladin, was markedly attenuated in HCFs transfected with the palladin siRNA compared with cells transfected with a control siRNA (Fig. 5C). These results thus suggested that the upregulation of palladin expression is required, at least in part, for the upregulation of α-SMA expression by TGF-β.

Effect of Palladin Depletion on TGF-β–Induced Collagen Gel Contraction Mediated by HCFs

Finally, to examine further the physiological role of palladin in corneal fibroblasts, we evaluated the effect of palladin depletion on collagen gel contraction mediated by HCFs. Exposure of HCFs cultured in a three-dimensional collagen gel to TGF-β resulted in a marked increase in the extent of gel contraction. Although this effect of TGF-β was inhibited slightly by prior transfection of the cells with a control siRNA, it was essentially prevented by transfection with the palladin siRNA (Fig. 6). These data thus suggested that palladin is required for HCF-mediated collagen gel contraction in response to stimulation with TGF-β.

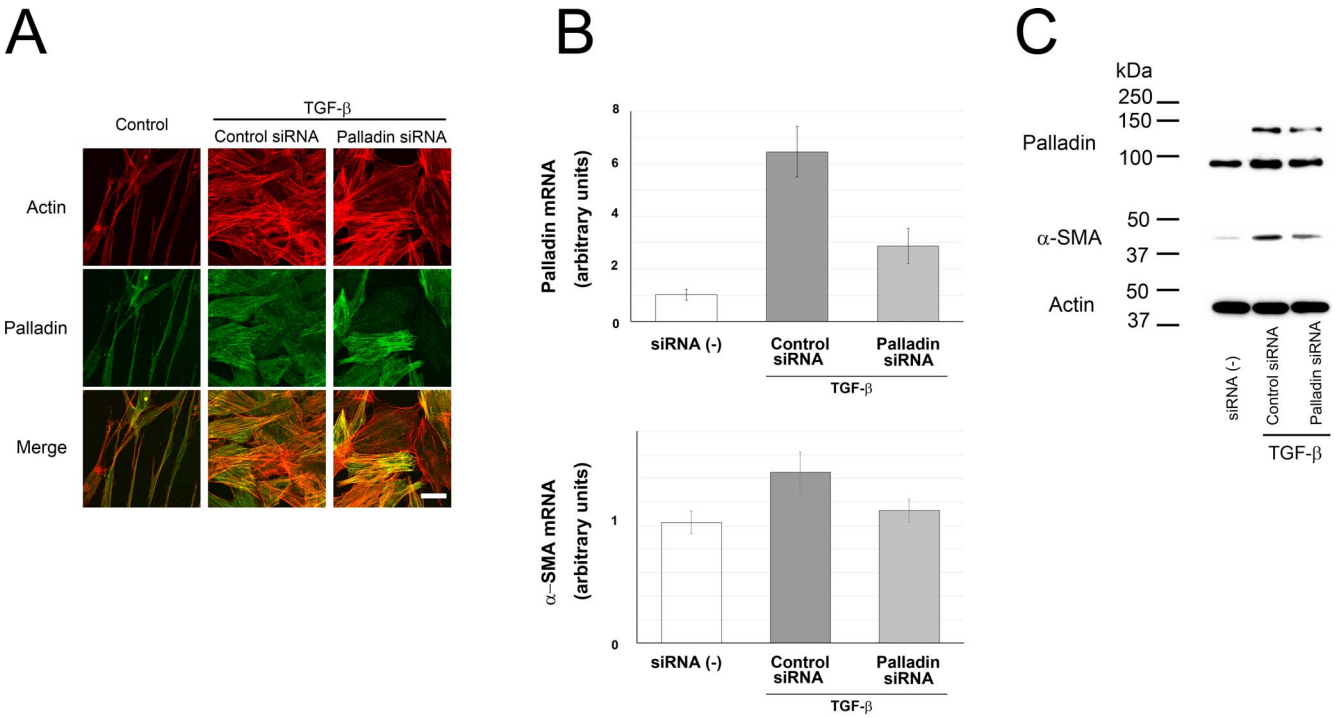

FIGURE 5. Effect of palladin depletion on the TGF-β–induced upregulation of α-SMA expression in HCFs. (**A**) Immunofluorescence analysis of palladin expression (*green fluorescence*) in HCFs transfected (or not) with control or palladin siRNAs and then incubated in the absence or presence of TGF-β (10 ng/mL) for 48 hours. The cells were also stained with rhodamine-phalloidin (*red fluorescence*) to detect the actin cytoskeleton. *Scale bar*: 50 μm. (**B**) Quantitative RT-PCR analysis of palladin and α-SMA mRNAs in HCFs transfected (or not) with control or palladin siRNAs and then incubated in the absence or presence of TGF-β (10 ng/mL) for 12 hours. Data are means ± SEM from three independent experiments. (**C**) Immunoblot analysis of palladin and α-SMA in HCFs transfected (or not) with control or palladin siRNAs and then incubated in the absence or presence of TGF-β (10 ng/mL) for 48 hours.

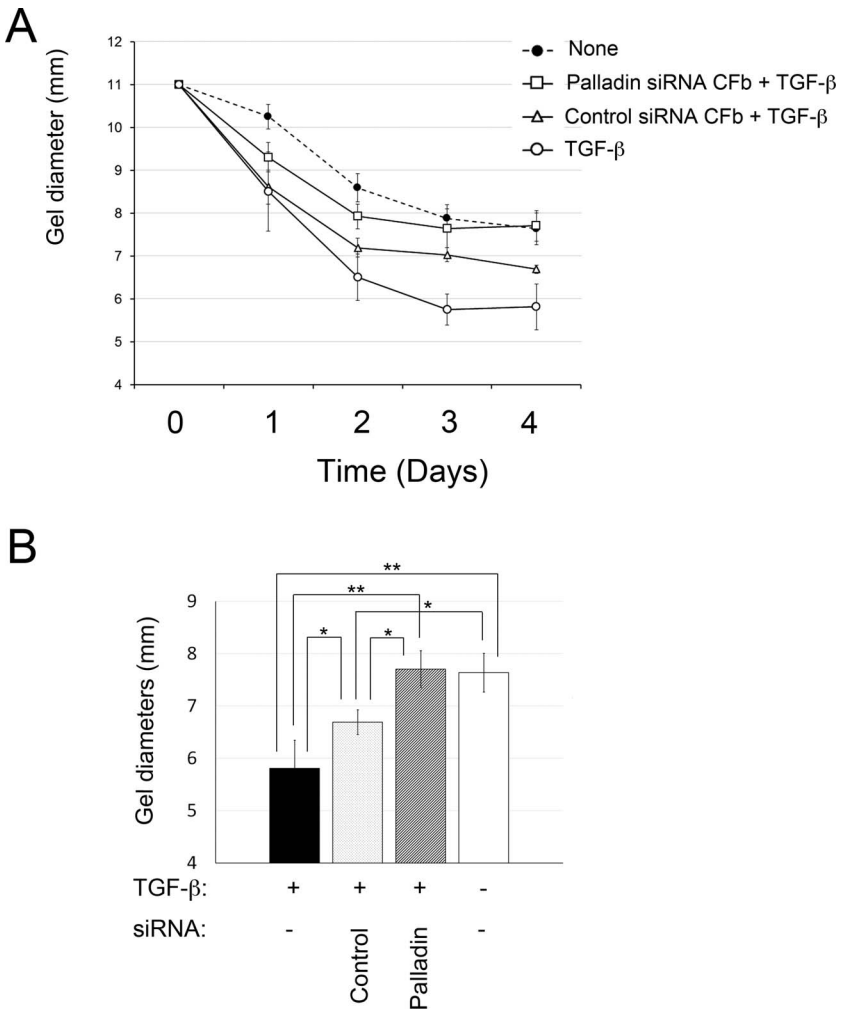

Figure 6. Effect of palladin depletion on TGF-β–induced collagen gel contraction mediated by HCFs. (**A**) Time course of collagen gel contraction mediated by HCFs transfected (or not) with control or palladin siRNAs and then incubated in the absence or presence of TGF-β (10 ng/mL). (**B**) Comparison of collagen gel diameter for cells incubated as in (**A**) for 4 days. All data are means ± SEM from three independent experiments. $^{*}P < 0.05$, $^{**}P < 0.0001$ (Tukey test). NS, not significant.

Discussion

We have here demonstrated the expression of palladin in HCFs, in the diseased human cornea, and in the wounded rat cornea and shown that the expression of palladin appeared to be closely related to that of α-SMA both in vitro and in vivo. The expression of palladin, especially the 140-kDa isoform, was upregulated in HCFs by TGF-β, and this effect appeared to be mediated in part by Smads or MAPK signaling. Finally, we found that the TGF-β–induced upregulation of α-SMA expression in HCFs as well as of cell contractility was dependent at least in part on the associated upregulation of palladin expression. Our results thus suggest that palladin is a potential target for therapeutic inhibition of scar formation in the corneal stroma.

The 140-kDa isoform of palladin is widely expressed in mammalian organs including the heart, stomach, bone, and uterus.[25,31] Multiple isoforms of palladin, including those with molecular sizes of 90, 140, and 200 kDa, have also been detected during mouse development,[25] with expression of the 140-kDa isoform beginning at embryonic day 7.5 and remaining evident in the brain, lung, kidney, colon, intestine, thymus, uterus, bladder, and ovary of adult animals.[25] The 140-kDa isoform of palladin is also expressed in TGF-β–stimulated human skin fibroblasts as well as in granular tissue of wounded human skin.[39] We have now shown that TGF-β induced expression of the 140-kDa isoform of palladin in HCFs in association with the upregulation of α-SMA. Given that skin and the cornea share an ectodermal origin, the expression of palladin might be similarly regulated in the two tissues. With regard to the biological role of palladin in the corneal stroma, we have now shown that the RNAi-mediated depletion of palladin in HCFs attenuated the TGF-β–induced increase both in the abundance of α-SMA and in cell contractility, suggesting that palladin may mediate these effects of TGF-β.

The expression of palladin was not detected in the normal human cornea, but it was apparent in diseased corneas as well as at the lesion site in a rat model of stromal wound healing. The expression of α-SMA is associated with scar formation in the cornea,[1,17] and we found that the expression of palladin in both the diseased cornea and the wounded cornea tended to overlap with that of α-SMA. Transforming growth factor–β[40] and its signaling pathways,[41] including those mediated by the MAPKs ERK, p38, and JNK, also play an important role in the formation of corneal stromal scars. Consistent with these previous observations, we have now found that TGF-β stimulated the expression of both palladin and α-SMA in HCFs in a manner dependent in part on p38, ERK, and JNK signaling,

although the Smad, JNK, or p38 pathway appeared to contribute to a greater extent than the ERK pathway to the regulation of palladin expression. Furthermore, RNAi-mediated depletion of palladin attenuated the TGF-β–induced increase in α-SMA expression. Together, our observations thus indicate that the expression of palladin in HCFs in vitro or in the corneal stroma in vivo is related to that of α-SMA as a marker of corneal stromal scarring and that palladin may mediate in part the TGF-β–induced expression of α-SMA in corneal fibroblasts.

We detected the colocalization of palladin and α-SMA in the diseased human cornea. Expression of α-SMA has previously been detected in the scarred,[19] keratoconic,[19] or bullous keratopathic cornea[19,20] and has been considered a marker for corneal scarring.[17] Whereas the expression of α-SMA was not previously detected in a specimen of corneal leukoma due to syphilitic interstitial keratitis,[42] it was apparent in the specimen of the cornea affected by this condition that was also positive for palladin in the present study. Given that TGF-β signaling is implicated in corneal scar formation, inhibition of such signaling has been pursued as a potential treatment for corneal scarring.[36,40,43,44] Current treatments for corneal scarring are limited to the topical administration of steroids, mitomycin, or tranilast. We have now shown that depletion of palladin by RNAi inhibited the TGF-β–induced expression of α-SMA in HCFs as well as collagen gel contraction mediated by these cells. Such collagen gel contraction mediated by corneal fibroblasts might be related to corneal scar formation, given that both processes have been found to be inhibited by rapamycin.[45] Our results now suggest that inhibition of palladin expression or function is also a potential approach to the treatment of corneal scarring.

In conclusion, the actin cytoskeleton–associated protein palladin was not detected in the normal cornea, but its expression was induced in association with scarring in both the human and rat cornea. The expression of palladin in HCFs was upregulated by TGF-β in a manner dependent on Smad and MAPK signaling and may contribute to the TGF-β–induced upregulation of α-SMA and contractility in these cells. Further investigation is thus warranted to shed light on the role of palladin in corneal stromal wound healing and scar formation.

Acknowledgments

The authors thank Yukari Mizuno for technical assistance.

Supported by Japan Society for the Promotion of Science KAKENHI Grant 25462716.

Disclosure: **N. Morishige**, None; **S. Murata**, None; **Y. Nakamura**, Senju Co. Ltd. (E); **H. Azumi**, None; **R. Shin-gyou-uchi**, None; **K.-T. Oki**, None; **Y. Morita**, None; **K.-H. Sonoda**, None

References

1. Jester JV, Huang J, Petroll WM, Cavanagh HD. TGFbeta induced myofibroblast differentiation of rabbit keratocytes requires synergistic TGFbeta, PDGF and integrin signaling. *Exp Eye Res*. 2002;75:645–657.
2. Jester JV, Petroll WM, Barry PA, Cavanagh HD. Expression of alpha-smooth muscle (alpha-SM) actin during corneal stromal wound healing. *Invest Ophthalmol Vis Sci*. 1995;36:809–819.
3. Kaur H, Chaurasia SS, de Medeiros FW, et al. Corneal stroma PDGF blockade and myofibroblast development. *Exp Eye Res*. 2009;88:960–965.
4. Maltseva O, Folger P, Zekaria D, Petridou S, Masur SK. Fibroblast growth factor reversal of the corneal myofibroblast phenotype. *Invest Ophthalmol Vis Sci*. 2001;42:2490–2495.
5. Jester JV, Barry-Lane PA, Cavanagh HD, Petroll WM. Induction of alpha-smooth muscle actin expression and myofibroblast transformation in cultured corneal keratocytes. *Cornea*. 1996; 15:505–516.
6. Desmouliere A, Geinoz A, Gabbiani F, Gabbiani G. Transforming growth factor-beta 1 induces alpha-smooth muscle actin expression in granulation tissue myofibroblasts and in quiescent and growing cultured fibroblasts. *J Cell Biol*. 1993; 122:103–111.
7. Hashimoto S, Gon Y, Takeshita I, Matsumoto K, Maruoka S, Horie T. Transforming growth Factor-beta1 induces phenotypic modulation of human lung fibroblasts to myofibroblast through a c-Jun-NH2-terminal kinase-dependent pathway. *Am J Respir Crit Care Med*. 2001;163:152–157.
8. Utsugi M, Dobashi K, Ishizuka T, et al. C-Jun-NH2-terminal kinase mediates expression of connective tissue growth factor induced by transforming growth factor-beta1 in human lung fibroblasts. *Am J Respir Cell Mol Biol*. 2003;28:754–761.
9. Lien SC, Usami S, Chien S, Chiu JJ. Phosphatidylinositol 3-kinase/Akt pathway is involved in transforming growth factor-beta1-induced phenotypic modulation of 10T1/2 cells to smooth muscle cells. *Cell Signal*. 2006;18:1270–1278.
10. Imamichi Y, Waidmann O, Hein R, Eleftheriou P, Giehl K, Menke A. TGF beta-induced focal complex formation in epithelial cells is mediated by activated ERK and JNK MAP kinases and is independent of Smad4. *Biol Chem*. 2005;386: 225–236.
11. Gao X, Li J, Huang H, Li X. Connective tissue growth factor stimulates renal cortical myofibroblast-like cell proliferation and matrix protein production. *Wound Repair Regen*. 2008; 16:408–415.
12. Karamichos D, Guo XQ, Hutcheon AE, Zieske JD. Human corneal fibrosis: an in vitro model. *Invest Ophthalmol Vis Sci*. 2010;51:1382–1388.
13. Ohji M, SundarRaj N, Thoft RA. Transforming growth factor-beta stimulates collagen and fibronectin synthesis by human corneal stromal fibroblasts in vitro. *Curr Eye Res*. 1993;12: 703–709.
14. Jester JV, Budge A, Fisher S, Huang J. Corneal keratocytes: phenotypic and species differences in abundant protein expression and in vitro light-scattering. *Invest Ophthalmol Vis Sci*. 2005;46:2369–2378.
15. Jester JV, Brown D, Pappa A, Vasiliou V. Myofibroblast differentiation modulates keratocyte crystallin protein expression, concentration, and cellular light scattering. *Invest Ophthalmol Vis Sci*. 2012;53:770–778.
16. Cockerham GC, Hidayat AA. Retrocorneal membrane with myofibroblasts after perforating injury: an immunohistochemical and ultrastructural study of 11 cases. *Cornea*. 1999;18: 700–706.
17. Jester JV, Petroll WM, Cavanagh HD. Corneal stromal wound healing in refractive surgery: the role of myofibroblasts. *Prog Retin Eye Res*. 1999;18:311–356.
18. Mohan RR, Hutcheon AE, Choi R, et al. Apoptosis, necrosis, proliferation, and myofibroblast generation in the stroma following LASIK and PRK. *Exp Eye Res*. 2003;76:71–87.
19. Kenney MC, Chwa M, Lin B, Huang GH, Ljubimov AV, Brown DJ. Identification of cell types in human diseased corneas. *Cornea*. 2001;20:309–316.
20. Morishige N, Nomi N, Morita Y, Nishida T. Immunohistofluorescence analysis of myofibroblast transdifferentiation in human corneas with bullous keratopathy. *Cornea*. 2011;30: 1129–1134.
21. Salmikangas P, Mykkanen OM, Gronholm M, Heiska L, Kere J, Carpen O. Myotilin, a novel sarcomeric protein with two Ig-like domains, is encoded by a candidate gene for limb-girdle muscular dystrophy. *Hum Mol Genet*. 1999;8:1329–1336.
22. Parast MM, Otey CA. Characterization of palladin, a novel protein localized to stress fibers and cell adhesions. *J Cell Biol*. 2000;150:643–656.

23. Bang ML, Mudry RE, McElhinny AS, et al. Myopalladin, a novel 145-kilodalton sarcomeric protein with multiple roles in Z-disc and I-band protein assemblies. *J Cell Biol*. 2001;153:413–427.
24. Mykkanen OM, Gronholm M, Ronty M, et al. Characterization of human palladin, a microfilament-associated protein. *Mol Biol Cell*. 2001;12:3060–3073.
25. Wang HV, Moser M. Comparative expression analysis of the murine palladin isoforms. *Dev Dyn*. 2008;237:3342–3351.
26. Boukhelifa M, Parast MM, Bear JE, Gertler FB, Otey CA. Palladin is a novel binding partner for Ena/VASP family members. *Cell Motil Cytoskeleton*. 2004;58:17–29.
27. Boukhelifa M, Moza M, Johansson T, et al. The proline-rich protein palladin is a binding partner for profilin. *FEBS J*. 2006; 273:26–33.
28. Ronty M, Taivainen A, Moza M, Kruh GD, Ehler E, Carpen O. Involvement of palladin and alpha-actinin in targeting of the Abl/Arg kinase adaptor ArgBP2 to the actin cytoskeleton. *Exp Cell Res*. 2005;310:88–98.
29. Ronty M, Taivainen A, Moza M, Otey CA, Carpen O. Molecular analysis of the interaction between palladin and alpha-actinin. *FEBS Lett*. 2004;566:30–34.
30. Luo H, Liu X, Wang F, et al. Disruption of palladin results in neural tube closure defects in mice. *Mol Cell Neurosci*. 2005; 29:507–515.
31. Rachlin AS, Otey CA. Identification of palladin isoforms and characterization of an isoform-specific interaction between Lasp-1 and palladin. *J Cell Sci*. 2006;119:995–1004.
32. Brentnall TA, Lai LA, Coleman J, Bronner MP, Pan S, Chen R. Arousal of cancer-associated stroma: overexpression of palladin activates fibroblasts to promote tumor invasion. *PLoS One*. 2012;7:e30219.
33. Cannon AR, Owen MK, Guerrero MS, et al. Palladin expression is a conserved characteristic of the desmoplastic tumor microenvironment and contributes to altered gene expression. *Cytoskeleton*. 2015;72:402–411.
34. Lucio PS, Cavalcanti AL, Alves PM, Godoy GP, Nonaka CF. Myofibroblasts and their relationship with oral squamous cell carcinoma. *Braz J Otorhinolaryngol*. 2013;79:112–118.
35. Kumagai N, Fukuda K, Ishimura Y, Nishida T. Synergistic induction of eotaxin expression in human keratocytes by TNF-alpha and IL-4 or IL-13. *Invest Ophthalmol Vis Sci*. 2000;41: 1448–1453.
36. Saika S, Ikeda K, Yamanaka O, et al. Expression of Smad7 in mouse eyes accelerates healing of corneal tissue after exposure to alkali. *Am J Pathol*. 2005;166:1405–1418.
37. Hayashida T, Decaestecker M, Schnaper HW. Cross-talk between ERK MAP kinase and Smad signaling pathways enhances TGF-beta-dependent responses in human mesangial cells. *FASEB J*. 2003;17:1576–1578.
38. Saika S. TGFbeta pathobiology in the eye. *Lab Invest*. 2006;86: 106–115.
39. Ronty MJ, Leivonen SK, Hinz B, et al. Isoform-specific regulation of the actin-organizing protein palladin during TGF-beta1-induced myofibroblast differentiation. *J Invest Dermatol*. 2006;126:2387–2396.
40. Jester JV, Barry-Lane PA, Petroll WM, Olsen DR, Cavanagh HD. Inhibition of corneal fibrosis by topical application of blocking antibodies to TGF beta in the rabbit. *Cornea*. 1997;16:177–187.
41. Shi L, Chang Y, Yang Y, Zhang Y, Yu FS, Wu X. Activation of JNK signaling mediates connective tissue growth factor expression and scar formation in corneal wound healing. *PLoS One*. 2012;7:e32128.
42. Kawaguchi R, Saika S, Wakayama M, Ooshima A, Ohnishi Y, Yabe H. Extracellular matrix components in a case of retrocorneal membrane associated with syphilitic interstitial keratitis. *Cornea*. 2001;20:100–103.
43. Mohan RR, Tandon A, Sharma A, Cowden JW, Tovey JC. Significant inhibition of corneal scarring in vivo with tissue-selective, targeted AAV5 decorin gene therapy. *Invest Ophthalmol Vis Sci*. 2011;52:4833–4841.
44. Saika S, Ikeda K, Yamanaka O, et al. Therapeutic effects of adenoviral gene transfer of bone morphogenic protein-7 on a corneal alkali injury model in mice. *Lab Invest*. 2005;85:474–486.
45. Milani BY, Milani FY, Park DW, et al. Rapamycin inhibits the production of myofibroblasts and reduces corneal scarring after photorefractive keratectomy. *Invest Ophthalmol Vis Sci*. 2013;54:7424–7430.

Investigative Ophthalmology & Visual Science